

# Intra-cellular transport of single-headed molecular motors KIF1A

Katsuhiko Nishinari,<sup>1</sup> Yasushi Okada,<sup>2</sup> Andreas Schadschneider,<sup>3</sup> and Debashish Chowdhury<sup>4</sup>

<sup>1</sup>*Department of Aeronautics and Astronautics, Faculty of Engineering,  
University of Tokyo, Hongo, Bunkyo-ku, Tokyo 113-8656, Japan.*

<sup>2</sup>*Department of Cell Biology and Anatomy, Graduate School of Medicine  
University of Tokyo, Hongo, Bunkyo-ku, Tokyo 113-0033, Japan.*

<sup>3</sup>*Institut für Theoretische Physik, Universität zu Köln D-50937 Köln, Germany*

<sup>4</sup>*Department of Physics, Indian Institute of Technology, Kanpur 208016, India.*

(Dated: November 20, 2018)

Motivated by experiments on single-headed kinesin KIF1A, we develop a model of intra-cellular transport by interacting molecular motors. It captures explicitly not only the effects of ATP hydrolysis, but also the ratchet mechanism which drives individual motors. Our model accounts for the experimentally observed single molecule properties in the low density limit and also predicts a phase diagram that shows the influence of hydrolysis and Langmuir kinetics on the collective spatio-temporal organization of the motors. Finally, we provide experimental evidence for the existence of domain walls in our *in-vitro* experiment with fluorescently labeled KIF1A.

PACS numbers: 87.16.Nn, 45.70.Vn, 02.50.Ey, 05.40.-a

Intra-cellular transport of a wide variety of cargo in eucaryotic cells is made possible by motor proteins, like kinesin and dynein, which move on filamentary tracks called microtubules (MT) [1, 2]. However, often a single MT is used simultaneously by many motors and, in such circumstances, the inter-motor interactions cannot be ignored. Fundamental understanding of these collective physical phenomena may also expose the causes of motor-related diseases (e.g., Alzheimer’s disease) [3] thereby helping, possibly, also in their control and cure. Some of the most recent theoretical models of interacting molecular motors [4, 5, 6, 7] utilize the similarities between molecular motor traffic on MT and vehicular traffic on highways [8] both of which can be modelled by appropriate extensions of driven diffusive lattice gases [9, 10]. In those models the motor is represented by a self-driven particle and the dynamics of the model is essentially an extension of that of the asymmetric simple exclusion processes (ASEP) [9, 10] that includes Langmuir-like kinetics of adsorption and desorption of the motors. In reality, a motor protein is an enzyme whose mechanical movement is loosely coupled with its biochemical cycle. In this letter we consider specifically the *single-headed* kinesin motor, KIF1A [11, 12, 13, 14]; the movement of a single KIF1A motor has been modelled recently with a Brownian ratchet mechanism [15, 16]. In contrast to the earlier models [4, 5, 6, 7] of molecular motor traffic, which take into account only the mutual interactions of the motors, our model explicitly incorporates also the Brownian ratchet mechanism of individual KIF1A motors, including its biochemical cycle that involves *adenosine triphosphate(ATP) hydrolysis*.

The ASEP-like models successfully explain the occurrence of shocks. But since most of the bio-chemistry is captured in these models through a single effective hopping rate, it is difficult to make direct quantitative comparison with experimental data which depend on such chemical processes. In contrast, the model we propose

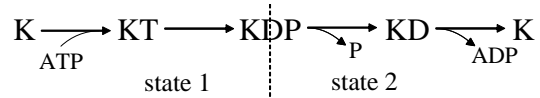


FIG. 1: The biochemical and mechanical states of a single KIF1A motor. On the left of the dotted line, KIF1A is bound to a fixed position on the MT (state 1), while on the right it diffuses along the MT track (state 2). At the transition from state 1 to 2, KIF1A detaches from the MT.

incorporates the essential steps in the biochemical processes of KIF1A as well as their mutual interactions and involves parameters that have one-to-one correspondence with experimentally controllable quantities.

The biochemical processes of kinesin-type molecular motors can be described by the four states model shown in Fig. 1 [11, 14]: bare kinesin (K), kinesin bound with ATP (KT), kinesin bound with the products of hydrolysis, i.e., adenosine diphosphate(ADP) and phosphate (KDP), and, finally, kinesin bound with ADP (KD) after releasing phosphate. Recent experiments [11, 14] revealed that both K and KT bind to the MT in a stereotypic manner (historically called “strongly bound state”, and here we refer to this mechanical state as “state 1”). KDP has a very short lifetime and the release of phosphate transiently detaches kinesin from MT [14]. Then, KD re-binds to the MT and executes Brownian motion along the track (historically called “weakly bound state”, and here referred to as “state 2”). Finally, KD releases ADP when it steps forward to the next binding site on the MT utilizing a Brownian ratchet mechanism, and thereby returns to the state K.

*Model definition.* — A single protofilament of MT is modelled by a one-dimensional lattice of  $L$  sites each of which corresponds to one KIF1A-binding site on the MT; the lattice spacing is equivalent to 8 nm which is the sep-

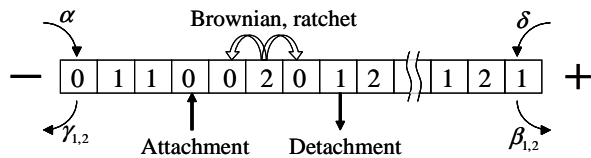


FIG. 2: A 3-state model for molecular motors moving along a MT. 0 denotes an empty site, 1 is K or KT and 2 is KD. Transition from 1 to 2, corresponding to hydrolysis, occurs within a site whereas movement to the forward or backward site occurs only when motor is in state 2. At the minus and plus ends the probabilities are different from those in the bulk.

aration between the successive binding sites on a MT [1]. Each kinesin is represented by a particle with two possible internal states labelled by the indices 1 and 2. Attachment of a motor to the MT occurs stochastically whenever a binding site on the latter is empty. Attachment and detachment at the two ends of the lattice need careful treatment and will be specified below. Thus, each of the lattice sites can be in one of three possible allowed states (Fig. 2): empty (denoted by 0), occupied by a kinesin in state 1, or occupied by a kinesin in state 2.

For the dynamical evolution of the system, one of the  $L$  sites is picked up randomly and updated according to the rules given below together with the corresponding probabilities (Fig. 2):

$$\text{Attachment : } 0 \rightarrow 1 \text{ with } \omega_a dt \quad (1)$$

$$\text{Detachment : } 1 \rightarrow 0 \text{ with } \omega_d dt \quad (2)$$

$$\text{Hydrolysis : } 1 \rightarrow 2 \text{ with } \omega_h dt \quad (3)$$

$$\text{Ratchet : } \begin{cases} 2 \rightarrow 1 \text{ with } \omega_s dt \\ 20 \rightarrow 01 \text{ with } \omega_f dt \end{cases} \quad (4)$$

$$\text{Brownian motion : } \begin{cases} 20 \rightarrow 02 \text{ with } \omega_b dt \\ 02 \rightarrow 20 \text{ with } \omega_b dt \end{cases} \quad (5)$$

The probabilities of detachment and attachment at the two ends of the MT may be different from those at any bulk site. We choose  $\alpha$  and  $\delta$ , instead of  $\omega_a$ , as the probabilities of attachment at the left and right ends, respectively. Similarly, we take  $\gamma_1$  and  $\beta_1$ , instead of  $\omega_d$ , as probabilities of detachments at the two ends (Fig. 2). Finally,  $\gamma_2$  and  $\beta_2$ , instead of  $\omega_b$ , are the probabilities of exit of the motors through the two ends by random Brownian movements.

Let us relate the rate constants  $\omega_f$ ,  $\omega_s$  and  $\omega_b$  with the corresponding physical processes in the Brownian ratchet mechanism of a single KIF1A motor. Suppose, just like models of flashing ratchets [15, 16], the motor “sees” a time-dependent effective potential which, over each biochemical cycle, switches back and forth between (i) a periodic but asymmetric sawtooth like form and (ii) a constant. The rate constant  $\omega_h$  in our model corresponds to the rate of the transition of the potential from the form (i) to the form (ii). The transition from (i) to (ii) happens soon after ATP hydrolysis, while the transition from (ii)

to (i) happens when ATP attaches to a bare kinesin [11]. The rate constant  $\omega_b$  of the motor in state 2 captures the Brownian motion of the free particle subjected to the flat potential (ii). The rate constants  $\omega_s$  and  $\omega_f$  are proportional to the overlaps of the Gaussian probability distribution of the free Brownian particle with, respectively, the original well and the well immediately in front of the original well of the sawtooth potential.

Let us denote the probabilities of finding a KIF1A molecule in the states 1 and 2 at the lattice site  $i$  at time  $t$  by the symbols  $r_i$  and  $h_i$ , respectively. In mean-field approximation the master equations for the dynamics of motors in the bulk of the system are given by

$$\frac{dr_i}{dt} = \omega_a(1 - r_i - h_i) - \omega_h r_i - \omega_d r_i + \omega_s h_i + \omega_f h_{i-1}(1 - r_i - h_i), \quad (6)$$

$$\frac{dh_i}{dt} = -\omega_s h_i + \omega_h r_i - \omega_f h_i(1 - r_{i+1} - h_{i+1}) - \omega_b h_i(2 - r_{i+1} - h_{i+1} - r_{i-1} - h_{i-1}) + \omega_b(h_{i-1} + h_{i+1})(1 - r_i - h_i). \quad (7)$$

The corresponding equations for the boundaries, which depend on the rate constants  $\alpha$ ,  $\delta$ ,  $\gamma_i$  and  $\beta_i$  for entry and exit (Fig. 2), are similar and will be presented elsewhere [13].

From experimental data [11, 12], good estimates for the parameters of the suggested model can be obtained. Assuming that one timestep corresponds to 1 ms, each simulation run had a duration of 1 minute in real time. The length of MT is fixed as  $L = 600$ . The detachment rate  $\omega_d \simeq 0.0001 \text{ ms}^{-1}$  is found to be independent of the kinesin population. On the other hand,  $\omega_a = 10^7 \text{ C/M}\cdot\text{s}$  depends on the concentration  $C$  (in M) of the kinesin motors. In typical eucaryotic cells *in-vivo* the kinesin concentration can vary between 10 and 1000 nM. Therefore, the allowed range of  $\omega_a$  is  $0.0001 \text{ ms}^{-1} \leq \omega_a \leq 0.01 \text{ ms}^{-1}$ . The rate  $\omega_b^{-1}$  must be such that the Brownian diffusion coefficient  $D$  in state 2 is of the order of  $40000 \text{ nm}^2/\text{s}$ ; using the relation  $\omega_b \sim D/(8\text{nm})^2$ , we get  $\omega_b \simeq 0.6 \text{ ms}^{-1}$ . Moreover, from the experimental observations that  $\omega_f/\omega_s \simeq 3/8$  and  $\omega_s + \omega_f \simeq 0.2 \text{ ms}^{-1}$ , we get the individual estimates  $\omega_s \simeq 0.145 \text{ ms}^{-1}$  and  $\omega_f \simeq 0.055 \text{ ms}^{-1}$ . The experimental data on the Michaelis-Menten type kinetics of hydrolysis [1] suggest that

$$\omega_h^{-1} \simeq \left[ 4 + 9 \left( \frac{0.1 \text{ mM}}{\text{ATP concentration (in mM)}} \right) \right] \text{ms} \quad (8)$$

so that the allowed biologically relevant range of  $\omega_h$  is  $0 \leq \omega_h \leq 0.25 \text{ ms}^{-1}$ .

*Single-molecule properties.* — An important test for the model is provided by a quantitative comparison of the low density properties with empirical results. Single molecule experiments [11] on KIF1A have established that

(i)  $v$ , the mean speed of the kinesins, is about  $0.2 \text{ nm/ms}$

ATP (mM)	$\omega_h$ (1/ms)	$v$ (nm/ms)	$D/v$ (nm)	$\tau$ (s)
$\infty$	0.25	0.201	184.8	7.22
0.9	0.20	0.176	179.1	6.94
0.3375	0.15	0.153	188.2	6.98
0.15	0.10	0.124	178.7	6.62

TABLE I: Predicted transport properties from this model in the low-density limit for four different ATP densities.  $\tau$  is calculated by averaging the intervals between attachment and detachment of each KIF1A.

if the supply of ATP is sufficient, and that  $v$  decreases with the lowering of ATP concentration following a Michaelis-Menten type relation like (8);

(ii)  $D/v \sim 190$  nm, irrespective of the ATP concentration, where  $D$  is the diffusion constant;

(iii)  $\tau$ , the mean duration of the movement of a kinesin on the MT, is more than 5 s, irrespective of the ATP concentration.

The corresponding predictions of our model (see Table I) for  $\omega_a = \alpha = 1.0 \times 10^{-6} \text{ ms}^{-1}$ , which allows realization of the condition of low density of kinesins, are in excellent agreement with the experimental results.

*Collective properties.* — Assuming *periodic* boundary conditions, the solutions  $(r_i, h_i) = (r, h)$  of the mean-field equations (7) in the steady-state are found to be

$$r = \frac{-\Omega_h - \Omega_s - (\Omega_s - 1)K + \sqrt{D}}{2K(1 + K)}, \quad (9)$$

$$h = \frac{\Omega_h + \Omega_s + (\Omega_s + 1)K - \sqrt{D}}{2K} \quad (10)$$

where  $K = \omega_d/\omega_a$ ,  $\Omega_h = \omega_h/\omega_f$ ,  $\Omega_s = \omega_s/\omega_f$ , and

$$D = 4\Omega_s K(1 + K) + (\Omega_h + \Omega_s + (\Omega_s - 1)K)^2. \quad (11)$$

The probability of finding an empty binding site on a MT is  $Kr$  as the stationary solution satisfies the equation  $r + h + Kr = 1$ . The steady-state flux of the motors along their MT tracks is then given by  $J = \omega_f h(1 - r - h)$ . It is interesting to note that in the *low* ATP concentration limit ( $\omega_h \ll \omega_s \simeq \omega_f$ ) of our model, the flux of the motors is well approximated by  $J_{\text{low}} = q_{\text{eff}}\rho(1 - \rho)$ , which formally looks like the corresponding expression for the totally asymmetric exclusion process, where  $\rho$  is close to the Langmuir limit  $1/(1 + K)$  and,

$$q_{\text{eff}} = \frac{\omega_h(1 + K)}{\Omega_s(1 + K) + K} \quad (12)$$

as the effective hopping probability[13].

Although the system with periodic boundary conditions is fictitious, the results provide good estimates of the density and flux in the corresponding system with open boundary conditions, particularly, in the high  $\omega_a$  regime (Fig. 3) which corresponds to jammed traffic of kinesin on MT (see Fig. 4). We also see that, for a given  $\omega_a$ , the bulk density of motors in state 2 exceeds that of those in state 1 as  $\omega_h$  increases beyond a certain value.

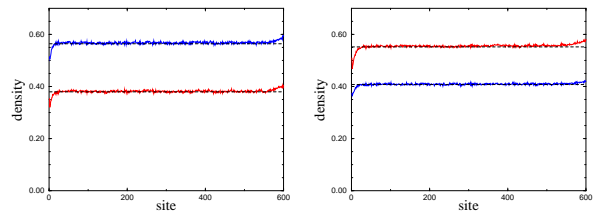


FIG. 3: The stationary density profiles for  $\omega_h = 0.1$  (left) and  $\omega_h = 0.2$  (right) in the case  $\omega_a = 0.001$ . The blue and red lines correspond to the densities of state 1 and 2, respectively. The dashed lines are the mean-field predictions (9) and (10) for periodic systems with the same parameters.

*Phase diagram.* — In contrast to the phase diagrams in the  $\alpha - \beta$ -plane reported by earlier investigators [4, 5, 6], we have drawn the phase diagram of our model (Fig. 4) in the  $\omega_a - \omega_h$  plane by carrying out extensive computer simulations for realistic parameter values of the model with open boundary conditions. The phase diagram shows the

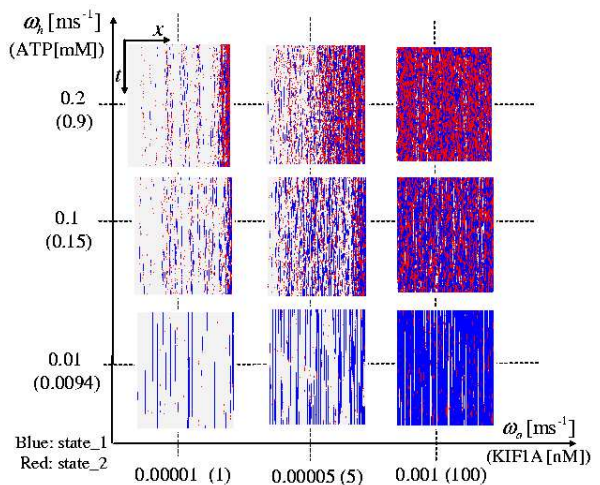


FIG. 4: Phase diagram of the model in the  $\omega_h - \omega_a$  plane, with the corresponding values for ATP and KIF1A concentrations given in brackets. These quantities are controllable in experiment. The boundary rates are  $\alpha = \omega_a, \beta_{1,2} = \omega_d, \gamma_{1,2} = \delta = 0$ . The position of the immobile shock depends on both ATP and KIF1A concentrations.

strong influence of hydrolysis on the spatial distribution of the motors along the MT. For very low  $\omega_h$  no kinesins can exist in state 2; the kinesins, all of which are in state 1, are distributed rather homogeneously over the entire system. In this case the only dynamics present is due to the Langmuir kinetics.

Even a small, but finite, rate  $\omega_h$  is sufficient to change this scenario. In this case both the density profiles  $\rho_j^1$  and  $\rho_j^2$  of kinesins in the states 1 and 2 exhibit a shock. As in the case of the ASEP-like models with Langmuir kinetics [5, 6], these shocks are localized. In computer simulations

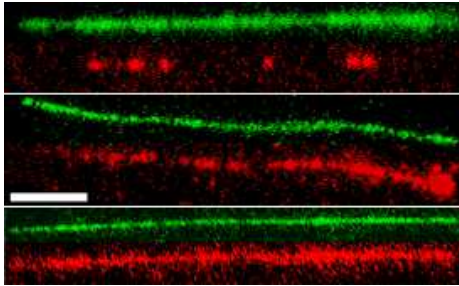


FIG. 5: Formation of comet-like accumulation of kinesin at the end of MT. Fluorescently labeled KIF1A (red) was introduced to MT (green) at 10 pM (top), 100 pM (middle) and 1000 pM (bottom) concentrations along with 2 mM ATP. The length of the white bar is  $2\mu\text{m}$ .

we have observed that the shocks in density profiles of kinesins in the states 1 and 2 always appear at the *same* position. Note that if the individual density profiles  $\rho_j^1$  and  $\rho_j^2$  exhibited shocks at two different locations, two shocks would appear in the *total* density profile  $\rho_j = \rho_j^1 + \rho_j^2$  violating the usual arguments [17] that ASEP-type models exhibit exactly one shock. Moreover, we have found that the position of the immobile shock depends on the concentration of the motors as well as that of ATP; the shock moves towards the minus end of the MT with the increase of the concentration of kinesin or ATP or both (Fig. 4).

Finally, we present direct experimental evidence that

support of the formation of the shock. The “comet-like structure”, shown in the middle of Fig. 5, is the collective pattern formed by the red fluorescent labelled kinesins where a domain wall separates the low-density region from the high-density region. The position of the domain wall depends on both ATP and KIF1A concentrations. Moreover, as we increase the concentration of KIF1A, the transition from the regime of free flow of kinesins to the formation of the shock is observed (top and middle in Fig. 5). Furthermore, we observe jammed traffic of kinesins at sufficiently high concentration (bottom in Fig. 5). The position of the shock in our simulation agrees well with the location of the domain wall in the comet-like structure observed in experiments [13].

In this letter we have developed a stochastic model for the collective intra-cellular transport by KIF1A motors, by taking into account the biochemical cycle of individual motors involving ATP hydrolysis and their mutual steric interactions. We have been able to identify the biologically relevant ranges of values of all the model parameters from the empirical data. In contrast to some earlier oversimplified models, the predictions of our model are in good quantitative agreement with the corresponding experimental data. Moreover, we have mapped the phase diagram of the model in a plane spanned by the concentrations of ATP and KIF1A, both of which are experimentally controllable quantities. Finally, we have reported the experimental observation of a comet-like collective pattern formed by the kinesin motors KIF1A and identified the domain wall in the pattern with the shock predicted by our model.

- 
- [1] J. Howard, *Mechanics of motor proteins and the cytoskeleton*, (Sinauer Associates, Sunderland, 2001) .
- [2] M. Schliwa (ed.), *Molecular Motors*, (Wiley-VCH, 2002).
- [3] N. Hirokawa and R. Takemura, *Trends in Biochem. Sci.* **28**, 558 (2003).
- [4] R. Lipowsky, S. Klumpp, and T. M. Nieuwenhuizen, *Phys. Rev. Lett.* **87**, 108101 (2001).
- [5] A. Parmeggiani, T. Franosch, and E. Frey, *Phys. Rev. Lett.* **90**, 086601 (2003); *Phys. Rev. E* **70**, 046101 (2004).
- [6] M.R. Evans, R. Juhasz, and L. Santen, *Phys. Rev. E* **68**, 026117 (2003); R. Juhasz and L. Santen, *J. Phys. A* **37**, 3933 (2004).
- [7] V. Popkov, A. Rakos, R.D. Williams, A.B. Kolomeisky, and G.M. Schütz, *Phys. Rev. E* **67**, 066117 (2003).
- [8] D. Chowdhury, L. Santen, and A. Schadschneider, *Phys. Rep.* **329**, 199 (2000); A. Schadschneider, *Physica A* **313**, 153 (2002).
- [9] B. Schmittmann and R.P.K. Zia, in C. Domb and J.L. Lebowitz (eds.), *Phase Transitions and Critical Phenomena*, Vol. 17 (Academic Press, 1995).
- [10] G.M. Schütz, in C. Domb and J.L. Lebowitz (eds.), *Phase Transitions and Critical Phenomena*, Vol. 19 (Academic Press, 2001).
- [11] Y. Okada and N. Hirokawa, *Science* **283**, 1152 (1999); *Proc. Natl. Acad. Sci. USA* **97**, 640 (2000).
- [12] Y. Okada, H. Higuchi, and N. Hirokawa, *Nature*, **424**, 574 (2003).
- [13] Y. Okada, K. Nishinari, D. Chowdhury, A. Schadschneider, and N. Hirokawa (to be published).
- [14] R. Nitta, M. Kikkawa, Y. Okada, and N. Hirokawa, *Science* **305**, 678 (2004).
- [15] F. Jülicher, A. Ajdari, and J. Prost, *Rev. Mod. Phys.* **69**, 1269 (1997).
- [16] P. Reimann, *Phys. Rep.* **361**, 57 (2002).
- [17] A.B. Kolomeisky, G. Schütz, E.B. Kolomeisky, and J.P. Straley, *J. Phys. A* **31**, 6911 (1998); V. Popkov and G.M. Schütz, *Europhys. Lett.* **48**, 257 (1999).